Analysis of DAR IMPATT Diode for Some Frequency Bands

ALEXANDER ZEMLIAK[1,3], FERNANDO REYES[2], JAIME CID[2], SERGIO VERGARA[2]
EVGENIY MACHUSSKIY[3]
[1]Department of Physics and Mathematics
[2]Department of Electronics
Autonomous University of Puebla
Av. San Claudio y Rio Verde, Puebla, 72570
MEXICO
[3]Institute of Technical Physics
National Technical University of Ukraine
UKRAINE
azemliak@fcfm.buap.mx

Abstract: - The analysis of DAR IMPATT diodes has been realized on basis of the precise drift-diffusion nonlinear model. The admittance characteristics of the DAR diode were analyzed in very wide frequency band from 30 up to 360 GHz. The energy characteristics have been optimized for the second high frequency band near the 220 GHz.

Key Words: - Active layer structure analysis, DAR IMPATT diode, high frequency band, implicit numerical scheme.

1 Introduction

The power generation in short part of millimeter region is one of the important problems of modern microwave electronics. The IMPATT diodes of different structures are used very frequently in microwave systems. The single drift region (SDR) and the double drift region (DDR) IMPATT diodes are very well known and used successfully for the microwave power generation in millimeter region [1-2]. From the famous paper of Read [3] the main idea to obtain the negative resistance was defined on the basis of the phase difference being produced between RF voltage and RF current due to delay in the avalanche build-up process and the transit time of charge carriers. However an IMPATT diode that has double avalanche regions (DAR) can produce an avalanche delay, which alone can satisfy conditions necessary to generate microwave power [4-7]. This diode can be defined for instance by means of the structure n+pνnp+ in Figure 1.

The characteristics of this diode were analyzed in [7] by means of approximate model. The authors affirm that the diode active properties are produced in many frequency bands for any drift zone width.

Our preliminary analysis that was obtained on basis of the sufficiently precise model [8-9] contradicts to the results [7]. We obtained three active frequency regions for proposed diode. We have been optimized the DAR IMPATT diode for the second frequency band near 200 GHz.

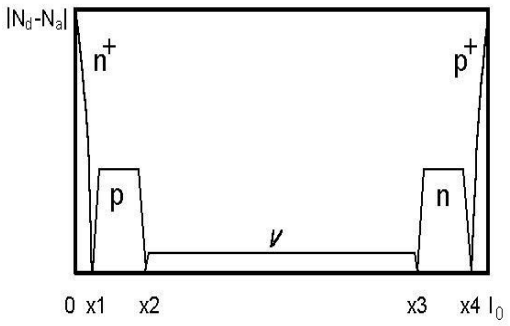

Figure 1. Doping profile of DAR IMPATT diode.

2 Nonlinear Model

The drift-diffusion model, which is used for the diode analysis, consists of two continuity equations for the electrons and holes, the Poisson equation for the potential distribution in semiconductor structure and necessary boundary conditions as for continuity equations and for the Poisson equation. The principal equations can be presented in next form:

$$\frac{\partial n(x,t)}{\partial t} = \frac{\partial J_n(x,t)}{\partial x} + \alpha_n \left| J_n(x,t) \right| + \alpha_p \left| J_p(x,t) \right|$$
$$\frac{\partial p(x,t)}{\partial t} = -\frac{\partial J_p(x,t)}{\partial x} + \alpha_n \left| J_n(x,t) \right| + \alpha_p \left| J_p(x,t) \right| \quad (1)$$

where

$$J_n(x,t) = n(x,t)\ V_n + D_n \frac{\partial\ n(x,t)}{\partial\ x}$$

$$J_p(x,t) = p(x,t)\ V_p - D_p \frac{\partial\ p(x,t)}{\partial\ x}$$

n, p are the concentrations of electrons and holes; J_n, J_p are the current densities; α_n, α_p are the ionization coefficients; V_n, V_p are the drift velocities; D_n, D_p are the diffusion coefficients. The dependences of the ionization coefficients on field and temperature and charge transport properties have been approximated using the approach in [10-13].

The boundary conditions for this system include concentration and current definition for contact points and can be written as follows:

$$\begin{aligned} &n(0,t) = N_D(0); \qquad p(l_0,t) = N_A(l_0); \\ &J_n(l_0,t) = J_{ns}; \qquad J_p(0,t) = J_{ps}. \end{aligned} \tag{2}$$

where J_{ns}, J_{ps} are the electron current and the hole current for inversely biased *p-n* junction; $N_D(0)$, $N_A(l_0)$ are the concentrations of donors and acceptors at two end space points x = 0 and x = l_0; where l_0 is the length of the active layer of semiconductor structure.

The electrical field distribution in semiconductor structure can be obtained from the Poisson equation. As electron and hole concentrations are functions of the time, therefore, this equation is the time dependent too and time is the equation parameter. The Poisson equation for the above-defined problem has the following normalized form:

$$\frac{\partial E(x,t)}{\partial x} = -\frac{\partial^2 U(x,t)}{\partial x^2} = N_D(x) - N_A(x) + p(x,t) - n(x,t) \tag{3}$$

where $N_D(x)$, $N_A(x)$ are the concentrations of donors and acceptors accordingly, *U(x,t)* is the potential, *E(x,t)* is the electrical field. The boundary conditions for this equation are:

$$U(0,t) = 0; \ \ U(l_0,t) = U_0 + \sum_{m=1}^{M} U_m \sin\left(\omega m t + \varphi_m\right) \tag{4}$$

where U_0 is the DC voltage on diode contacts; U_m is the amplitude of harmonic number *m* in diode contacts; ω is the fundamental frequency; φ_m is the phase of harmonic number *m*; *M* is the number of harmonics. In this paper we analyze one harmonic regime only (*M=1*) and in this case the phase φ_m can be define as 0. Concrete values of the voltages U_0, U_1 and frequency ω have been defined during the analysis in section 4. Equations (1)-(4) adequately describe processes in the IMPATT diode in a wide frequency band. However, numerical solution of this system of equations is very difficult due to existing of a sharp dependence of equation coefficients on electric field. Explicit numerical schemes have poor stability and require a lot of computing time for good calculation accuracy obtaining [14]. It is more advantageous to use implicit numerical scheme that has a significant property of absolute stability. Computational efficiency and numerical algorithm accuracy are improved by applying the space and the time coordinates symmetric approximation.

After approximation of functions and its differentials the system (1) is transformed to the implicit modified Crank-Nicholson numerical scheme. This modification consists of two numerical systems each of them having three-diagonal matrix. These systems are defined by form:

$$\begin{aligned} &-(a_n - b_n)\ n_{i-1}^{k+1} + (1+2a_n)\ n_i^{k+1} - (a_n + b_n)\ n_{i+1}^{k+1} = \\ &\quad a_n\ n_{i-1}^{k} + (1-2a_n)\ n_i^{k} + a_n\ n_{i+1}^{k} + b_n\ \left(n_{i+1}^{k} - n_{i-1}^{k}\right) \\ &\qquad + \alpha_n \left|\tau \cdot V_n \cdot n_i^k + r \cdot D_n \cdot \left(n_{i+1}^k - n_{i-1}^k\right)\right| \\ &\qquad + \alpha_p \left|\tau \cdot V_p \cdot p_i^k - r \cdot D_p \cdot \left(p_{i+1}^k - p_{i-1}^k\right)\right| \\ &-(a_p + b_p)\ p_{i-1}^{k+1} + (1+2a_p)\ p_i^{k+1} - (a_p - b_p)\ p_{i+1}^{k+1} = \\ &\quad a_p\ p_{i-1}^{k} + (1-2a_p)\ p_i^{k} + a_p\ p_{i+1}^{k} - b_p\ \left(p_{i+1}^{k} - p_{i-1}^{k}\right) \\ &\qquad + \alpha_p \left|\tau \cdot V_p \cdot p_i^k - r \cdot D_p \cdot \left(p_{i+1}^k - p_{i-1}^k\right)\right| \\ &\qquad + \alpha_n \left|\tau \cdot V_n \cdot n_i^k + r \cdot D_n \cdot \left(n_{i+1}^k - n_{i-1}^k\right)\right| \end{aligned} \tag{5}$$

$i = 1, 2, \ldots \quad I_1 - 1; \qquad k = 0, 1, 2, \ldots \infty$

where $a_{n,p} = \frac{\tau\ D_{n,p}}{2h^2}$; $b_{n,p} = \frac{\tau\ V_{n,p}}{4h}$; $r = \frac{\tau}{2h}$; *i* is the space coordinate current node number; *k* is the time coordinate node number; *h* is the space step; τ is the time step; I_1 is the space node number.

The approximation of the Poisson equation is performed using ordinary finite difference scheme at every time step *k*:

$$U_{i-1}^k - 2U_i^k + U_{i+1}^k = h^2\left(N_{Di} - N_{Ai} + p_i^k - n_i^k\right) \tag{6}$$

Numerical algorithm for the calculation of IMPATT diode characteristics consists of the following stages: 1) the voltage is calculated at the diode contacts for every time step by formula (4); 2) the voltage distribution is calculated at every space point from the Poisson equation (6) by factorization method [15], the electrical field distribution along the diode active layer is calculated; 3) the charge carries ionization and drift parameters are calculated in numerical net nodes for the current time step; 4) the system of equations (5) is solved by matrix factorization method taking into account the boundary conditions (2) and electron and hole concentration distributions are calculated for the new time step and then the calculation cycle is repeated for all time steps until the end of the time period; 5) the full current in external circuit is calculated. This process is continued from one period to another until the convergence is achieved by means of the results comparison for the two neighboring periods with the necessary precision. Then all harmonics of the external current, admittance for the harmonic number *m* and power characteristics can be calculated by the Fourier transformation.

3 Optimization Technique

The special optimization algorithm that combines one kind of direct method and a gradient method was used to optimize the output characteristics of DAR diode. To obtain the better solution for the optimum procedure, it is necessary to analyze *N*-dimensional space for *N*=5. The principal vector of optimization parameters consists of five variables $y = (y_1, y_2, y_3, y_4, y_5)$, where the components will be defined below. The optimization algorithm can be defined by next steps:

1. Given as input two different approximations of two initial points y^0 and y^1.

2. At these points, we start with the gradient method, and have performed some steps. As a result, we have two new points Y^0 and Y^1. This process is reflected by the next equations:

$$y^{0,n+1} = y^{0,n} - \delta_n \cdot \nabla F\left(y^{0,n}\right),$$

$$y^{1,n+1} = y^{1,n} - \delta_n \cdot \nabla F\left(y^{1,n}\right), \quad (7)$$

$$n=0,1,\ldots,N-1$$

$$Y^0 = y^{0,N}, \quad Y^1 = y^{1,N},$$

where F is the cost function, and, δ_n is the parameter of the gradient method.

3. We draw a line through two these points, and perform a large step along this line. We have a new point y^{s+1}:

$$y^{s+1} = Y^s + \alpha\left(Y^s - Y^{s-1}\right), \; s = 1, \quad (8)$$

where α is the parameter of the line step.

4. Then we perform some steps from this point by the gradient method, to obtain a new point Y^s:

$$y^{s,n+1} = y^{s,n} - \delta_n \cdot \nabla F\left(y^{s,n}\right), \quad (9)$$

$$s = s + 1, \; Y^s = y^{s,N}.$$

Then step 3 and 4 are repeated with the next values of index s (s = 2, 3,…).

This optimization algorithm cannot find the global maximum of the cost function, but only a local one. To obtain the better solution of the optimum procedure, it is necessary to analyze *N*-dimensional volume with different initial points. During the optimization process, it is very important to localize the subspace of the *N*-dimensional optimization space for more detailed analysis. Then this subspace can be analyzed carefully.

4 Numerical Scheme Convergence

The numerical scheme for the problem (1) for the DDR IMPATT diode structures was produced some years ago [16]. The scheme analysis showed a very good convergence of the numerical model. The numerical algorithm convergence was obtained during 6–8 high frequency periods. On the other hand the careful analysis of numerical model for the DAR diode with the doping profile in Figure 1 shows that the numerical scheme convergence for this type of the doping profile is very slow and the numerical transition process continues many periods to obtain the stationary mode (Figure 2).

The necessary number of the consequent periods depends on the diode width and operating frequency and changes from 30 – 50 for the frequency band 15 – 60 GHz up to 150 – 250 periods for 200 – 300 GHz. This very slow convergence was stipulated by the asynchronies movement of the electron and hole avalanches along the same drift region *v*. It occurs owing to the different drift velocities of the carriers. This effect provokes a large number of necessary periods and large computer time. This is a specific feature of the analyzed type of diode structure.

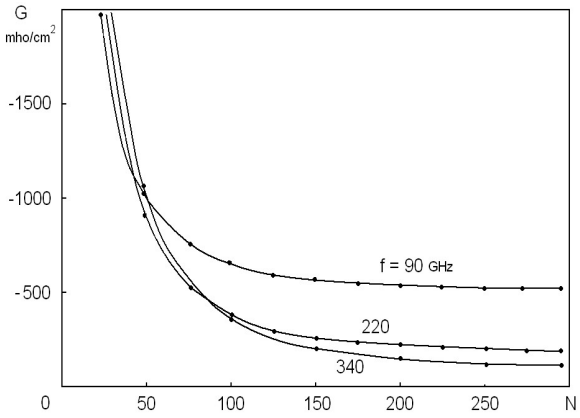

Figure 2. Calculated conductance as function of period number *N*.

5 Results and Discussion

5.1 Admittance characteristics of DAR diodes

The DDR type of IMPATT diode produces one frequency band only in practice because a very strong losses for high frequency bands.

The accurate analysis for DAR IMPATT diode has been made for different values of *p*, *n* and *v* region width and the different donor and acceptor concentration level. The analysis shows that the active properties of the diode practically are not displayed for more or less significant width of the region *v* [9]. The same doping profile as in [7] gives the negative conductance for very narrow frequency band only as shown in Figure 3 in conductance versus susceptance plot.

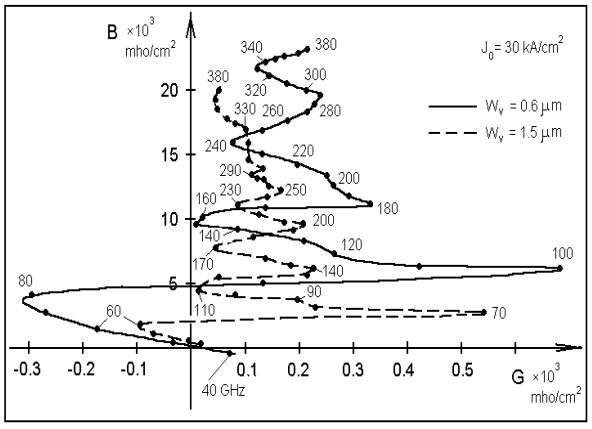

Figure 3. Complex small signal DAR diode admittance (conductance -*G* versus susceptance *B*) for different frequencies and two values of drift layer widths W_v.

The solid line of this figure gives dependency for drift layer width $W_v = 0.6\ \mu$m and the dash line for $W_v = 1.5\ \mu$m. First dependency displays the diode active properties for one narrow frequency band from 50 GHz up to 85 GHz. Second admittance dependency for $W_v = 1.5\ \mu$m gives very narrow one frequency band from 40 GHz up to 62 GHz with a very small value of negative conductance *G*. In general the admittance behavior has a damp oscillation character but only first peak lies in negative semi plane. The negative conductance disappears completely for $W_v > 1.5\ \mu$m.

The main reason of this effect is a non-synchronize mechanism of carriers' movement along the drift region. This conclusion is contrary to results of the paper [7]. Our results display the active features of the DAR diode the same profile for some frequency bands when the *v*-region width less than $0.5\ \mu$m.

One positive idea to increase negative admittance of the diode consists in non-symmetric doping profile utilization. This profile gives some compensation to the asynchronies mechanism. One of the perspective diode structures that was analyzed detail is defined by means of following parameters: the doping level for *n* and *p* zone is equal to $0.5_{10}17$ cm^{-3} and $0.2_{10}17$ cm^{-3}, accordingly, the widths of the two corresponding areas are equal to $0.1\ \mu$m and $0.2\ \mu$m, the width of the drift *v*-region is equal to $0.32\ \mu$m. In Figure 4 the small signal complex admittance i.e. the conductance versus susceptance is presented for the current density $J_0 = 30$ kA/cm^2. It is clear that we can obtain larger value of the conductance increasing the current density.

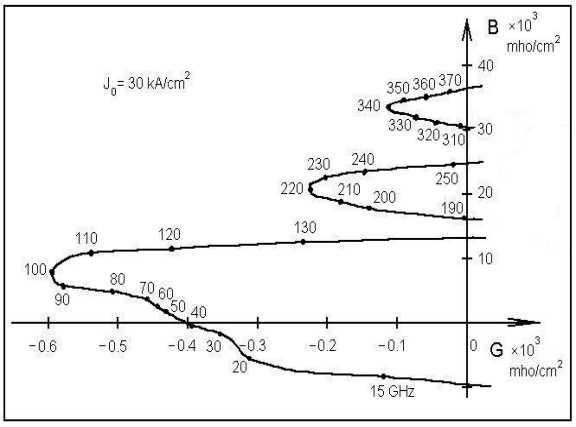

Figure 4. Complex small signal DAR diode admittance for different frequencies and $W_v = 0.32\ \mu$m.

We can decide that two superior bands appear from the positive conductance *G* semi plane (look Figure 3) as a result of the special conditions making for these bands. This effect gives possibility to use superior frequency bands, at least the second band, for the microwave power generation of the sufficient level.

We can decide that two superior bands appear as a result of the special conditions making for these bands. This effect gives possibility to use the second and the third bands for the microwave power generation of the sufficient level.

5.2 DAR diode optimization for 220 GHz

The DAR diode internal structure optimization has been provided for the second frequency band near 220 GHz for the feeding current density 30 kA/cm^2. The cost function of the optimization process was selected as output power level for the frequency 220 GHz. The set of the variables for the optimization procedure was composed from five technological parameters of the diode structure: two doping levels for *p* and *n* regions and three widths of *p*, *n* and *v* regions. The optimal values of these parameters were found: doping levels of *n* and *p* zone are equal to 0.42 $_{10}$17 cm^{-3} and 0.28$_{10}$17 cm^{-3} accordingly, the widths of the two corresponding areas are equal to 0.1 μm and 0.2 μm, and the width of the drift *v*-region is equal to 0.34 μm. The results of the complete analysis for three current density values 30, 50 and 70 kA/cm^2 are shown in Figure 5. The active diode properties for two first bands are improved when the current density increases. More positive effect was obtained for the frequency 220 GHz because the optimization for this frequency.

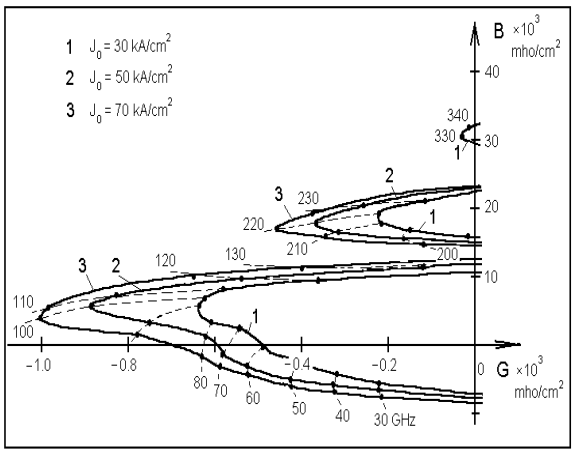

Figure 5. Complex small signal DAR diode admittance optimized for second frequency band for different value of feeding current.

The characteristics obtained for 220 GHz under a large signal serve as the main result. The amplitude characteristics for the conductance and the output power for this frequency are shown in Figure 6 and Figure 7 accordingly, for three values of the current density.

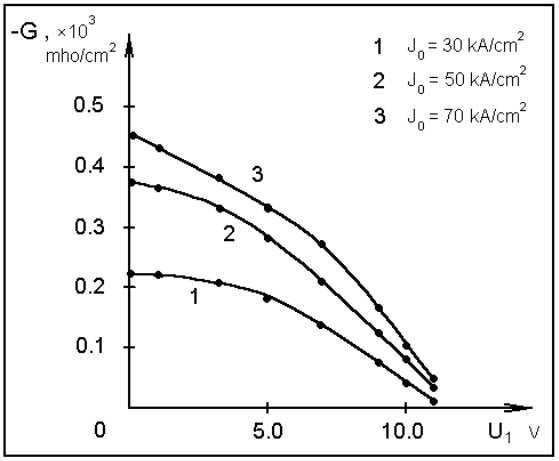

Figure 6. Conductance *G* dependency as function of first harmonic amplitude U_1 for 220 GHz.

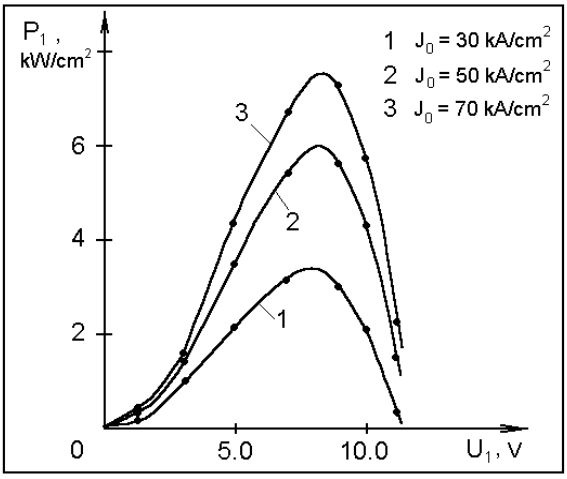

Figure 7. Output generated power *P* dependency as function of first harmonic amplitude U_1 for 220GHz.

We can state that a sufficient improvement of power characteristics is observed for this diode structure in comparison with non optimized structure. The maximum values of generated power are equal to 3.3 kW/cm^2 for J_0 =30 kA/cm^2, 6.0 kW/cm^2 for J_0 =50 kA/cm^2 and 7.5kW/cm^2 for J_0 =70 kA/cm^2 accordingly.

6 Conclusion

The numerical scheme that has been developed for the analysis of the different types of IMPATT diodes is suitable for the DAR complex doping profile investigation too. The additional problem that appears for the DAR diode structure analysis is the slower convergence of the numerical model in comparison with the DDR diode analysis.

Some new features of the DAR diode were obtained by the analysis on the basis of nonlinear model on comparing with DDR diode. The principal obtained results contradict to the data that were obtained before on the basis of the approximate models of the DAR diode. These results show that the diode does not have the active properties in some frequency bands for the sufficiently large drift region. To obtain the negative conductance for some frequency bands we need to reduce the drift layer widths to obtain W_v lesser than $0.5\,\mu$m. Nevertheless the diode has a wide first frequency band generation and two superior frequency bands with sufficient output power level. The diode structure optimization gives the possibility to increase the output power level for high frequency bands. This level can be exceeding by the special diode structure optimization taking into account necessary feeding current density.

Acknowledgement

This work was supported by the Autonomous University of Puebla by the project VIEP ZEEA/EXC/12-G.

References:

[1] G.I. Haddad, P.T. Greiling, and W.E. Schroeder, Basic principles and properties of avalanche transit-time devices, *IEEE Trans. Microwave Theory Tech.*, MTT-18, 1970, pp. 752-772.

[2] Chang K. (Ed.), *Handbook of microwave and optical components*, John Wile & Sons, N.Y., 1990.

[3] W.T. Read, A proposed high-frequency negative resistance diode, *Bell Syst Tech. J*, Vol. 37, 1958, pp. 401-446.

[4] B. Som, B.B.Pal, and S.K.Roy, A small signal analysis of an IMPATT device having two avalanche layers interspaced by a drift layer, *Solid-State Electron.,* Vol. 17, 1974, pp. 1029-1038.

[5] D.N. Datta, B.B.Pal, Generalized small signal analysis of a DAR IMPATT diode", *Solid-State Electron*, Vol. 25, No. 6, 1982, pp. 435-439.

[6] S.P. Pati, J.P. Banerjee, and S.K. Roy, High frequency numerical analysis of double avalanche region IMPATT diode, *Semicond Sci Technol*, No. 6, 1991, pp. 777-783.

[7] A.K. Panda, G.N. Dash, and S.P. Pati, Computer-aided studies on the wide-band microwave characteristics of a silicon double avalanche region diode, *Semicond Sci Technol*, No. 10, 1995, pp. 854-864.

[8] A. Zemliak, and R. De La Cruz, Comparative analysis of double drift region and double avalanche region IMPATT diodes, *WSEAS Trans. on Communications,* Vol. 3, No.1, 2004, p.22-27.

[9] A. M. Zemliak, S. Cabrera, Numerical Analysis of a DAR IMPATT diode, *J Comput Electron*, Vol. 5, No. 4, December 2006, pp. 401-404.

[10] W.N. Grant, Electron and hole ionization rates in epitaxial silicon at high electric fields, *Solid-State Electron*., Vol. 16, No. 10, 1973, pp. 1189-1203.

[11] C. Jacoboni, C. Canali, G. Ottaviani, A review of some charge transport properties of silicon, *Solid-State Electron*, Vol. 20, 1977, pp. 77-89.

[12] C. Canali, C. Jacoboni, G. Ottaviani, High field diffusion of electrons in silicon, *Appl Phys Lett*, Vol. 27, 1975, p. 278.

[13] F. Nava, C. Canali, L. Reggiani, D. Gasquet, J.C. Vaissiere, and J.P. Nougier, On diffusivity of holes in silicon, *J Appl Phys*, Vol. 50, 1979, p. 922.

[14] A.M. Zemliak, Difference scheme stability analysis for IMPATT-diode design, *Izv. VUZ Radioelectronika*, Vol. 24, No. 8, 1981, pp. 831-834.

[15] A. Zemliak, S. Khotiaintsev, and C. Celaya, Complex nonlinear model for the pulsed-mode IMPATT diode, *Instrumentation and Development*, Vol. 3, No. 8, 1997, pp. 45-52.

[16] A. Zemliak, C. Celaya, R. Garcia, Active layer parameter optimization for high-power Si 2 mm pulsed IMPATT diode, *Microwave Opt. Technol. Lett.*, Vol. 19, No. 1, 1998, pp. 4-9.